

LocInv: Localization-aware Inversion for Text-Guided Image Editing

Chuanming Tang*

University of Chinese Academy of Sciences
Computer Vision Center, Spain
tangchuanming19@mails.ucas.ac.cn

Kai Wang*

Computer Vision Center, Spain
kwang@cvc.uab.es

Fei Yang †

College of Computer Science
Nankai University
feiyang@nankai.edu.cn

Joost van de Weijer

Computer Vision Center, Spain
Universitat Autònoma de Barcelona
joost@cvc.uab.es

Abstract

Large-scale Text-to-Image (T2I) diffusion models demonstrate significant generation capabilities based on textual prompts. Based on the T2I diffusion models, text-guided image editing research aims to empower users to manipulate generated images by altering the text prompts. However, existing image editing techniques are prone to editing over unintentional regions that are beyond the intended target area, primarily due to inaccuracies in cross-attention maps. To address this problem, we propose **Localization-aware Inversion (LocInv)**, which exploits segmentation maps or bounding boxes as extra localization priors to refine the cross-attention maps in the denoising phases of the diffusion process. Through the dynamic updating of tokens corresponding to noun words in the textual input, we are compelling the cross-attention maps to closely align with the correct noun and adjective words in the text prompt. Based on this technique, we achieve fine-grained image editing over particular objects while preventing undesired changes to other regions. Our method LocInv, based on the publicly available Stable Diffusion, is extensively evaluated on a subset of the COCO dataset, and consistently obtains superior results both quantitatively and qualitatively.

1. Introduction

Text-to-Image (T2I) models have made remarkable progress and demonstrated an unprecedented ability to generate diverse and realistic images [35, 42, 47, 48, 63]. T2I models are trained on gigantic language-image datasets, ne-

cessitating significant computational resources. However, despite their impressive capabilities, they do not directly support *real image editing*, and they typically lack the capability to precisely control specific regions in the image.

Recent research on *text-guided image editing* allows users to manipulate an image using only text prompts [8, 17, 54, 60, 62]. In this paper, we focus on text-guided editing, where we aim to change the visual appearance of a specific source object in the image. Several of the existing methods [29, 37, 39, 52] use DDIM inversion [49] to attain the initial latent code of an image and then apply their proposed editing techniques along the denoising phase. Nonetheless, present text-guided editing methods are susceptible to inadvertent alterations of image regions. This arises from the heavy reliance of existing editing techniques on the precision of cross-attention maps. DPL [53] observes the phenomenon that the cross-attention maps from DDIM [49] and NTI [37] do not only correlate with the corresponding objects. This phenomenon is attributed to *cross-attention leakage*, which is the main factor impeding these image editing methods to work for complex *multi-object* images. To address this, DPL enhances the cross-attention by incorporating additional attention losses. However, DPL relies on a relatively weak connection between the noun and its associated object. This connection occasionally tends to be weak and results in unsatisfactory performance. Furthermore, given recent advancements in text-based segmentation and detection foundation models [27, 31, 58, 65], it is now straightforward to automatically obtain strong localization priors into general applications.

In this paper, we include localization priors to offer enhanced mitigation against *cross-attention leakage*. With the introduction of localization priors, our approach, named Localization-aware Inversion (*LocInv*), involves updating the token representations associated with objects at *each*

*Equal contributions

†Corresponding Author

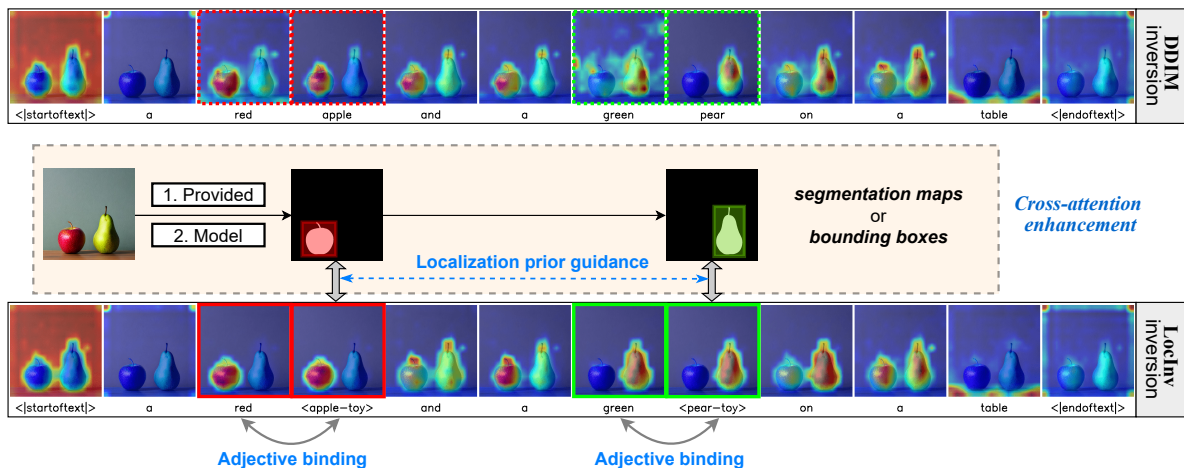


Figure 1. Compared with the naive DDIM inversion, our method *LocInv* aims at enhancing the cross-attention maps by applying localization priors (segmentation maps or detection bounding boxes provided by the datasets or foundation models) to guide the inversion processes. Furthermore, to force strong bindings between adjective and noun words, we constrain the cross-attention similarity between them.

timestep, a technique akin to *dynamic prompt learning* [53]. In both segmentation and detection scenarios, we optimize two losses—namely, the similarity loss and overlapping loss—to ensure that the cross-attention maps align closely with the provided priors. Moreover, to accommodate situations in which adjectives describe their associated noun words, we incorporate an additional similarity loss to reinforce the binding between them. In the experiments, we quantitatively evaluate the quality of cross-attention maps on a dataset *COCO-edit* collected from MS-COCO [30]. We further combine *LocInv* with P2P [18] to compare with other image editing methods. *LocInv* shows superior evaluation metrics and improved user evaluation. Furthermore, we qualitatively show prompt-editing results for Word-Swap and Attribute-Edit.

2. Related work

Inversion based editing is mainly relying on the DDIM inversion [49], which shows potential in editing tasks by deterministically calculating and encoding context information into a latent space and then reconstructing the original image using this latent representation. However, DDIM is found lacking for text-guided diffusion models when classifier-free guidance (CFG) [20] is applied, which is necessary for meaningful editing. Leveraging optimization on null-text embedding, Null-Text Inversion (NTI) [37] further improved the image reconstruction quality when CFG is applied and retained the rich text-guided editing capabilities of the Stable Diffusion model [45]. Negative-prompt inversion (NPI) [36] and ProxNPI [16] reduces the computation cost for the inversion step while generating similarly competitive reconstruction results as Null-text inversion. Direct Inversion [24] further enhances the inversion technique by adjusting the editing direction in each timestep to offer essential content preservation and edit fidelity. IterInv [50] gen-

eralizes the inversion to the DeepFloyd-IF T2I model [48].

Text-guided editing methods [3, 10, 26, 28, 29] of recent researches [23, 34, 40] in this topic adopt the large pre-trained text-to-image(T2I) models [7, 13, 21, 43, 44, 47] for controllable image editing. Among them, Imagic [25] and P2P [18] attempt structure-preserving editing via Stable Diffusion (SD) models. However, Imagic [25] requires fine-tuning the entire model for each image. P2P [18] has no need to fine-tune the model and retrain the image structure by assigning *cross-attention* maps from the original image to the edited one in the corresponding text token. InstructPix2Pix [4] is an extension of P2P by allowing human-like instructions for image editing. NTI [37] further makes the P2P capable of handling real images. Recently, pix2pix-zero [39] propose noise regularization and *cross-attention* guidance to retrain the structure of a given image. DiffEdit [11] automatically generates a mask highlighting regions of the input image by contrasting predictions conditioned on different text prompts. PnP [52] demonstrated that the image structure can be preserved by manipulating *spatial features* and *self-attention* maps in the T2I models.

There are also text-guided inpainting methods [15, 33, 38, 45] to achieve the editing purposes given user-specific masks. For example, Blended diffusion [1] adapts from a pre-trained unconditional diffusion model and encourages the output to align with the text prompt using the CLIP score. Blended latent diffusion (BLD) [2] further extend to the LDM [45]. Nonetheless, inpainting methods primarily concentrate on filling arbitrary objects in specified regions while ensuring visual coherence with the surrounding areas. These methods do not inherently preserve *semantic similarity* between the source and target objects, as is required for image translation effects.

Text-based segmentation and detection models aim at segmenting or detecting arbitrary classes with the help of language generalization property after pretraining. One of

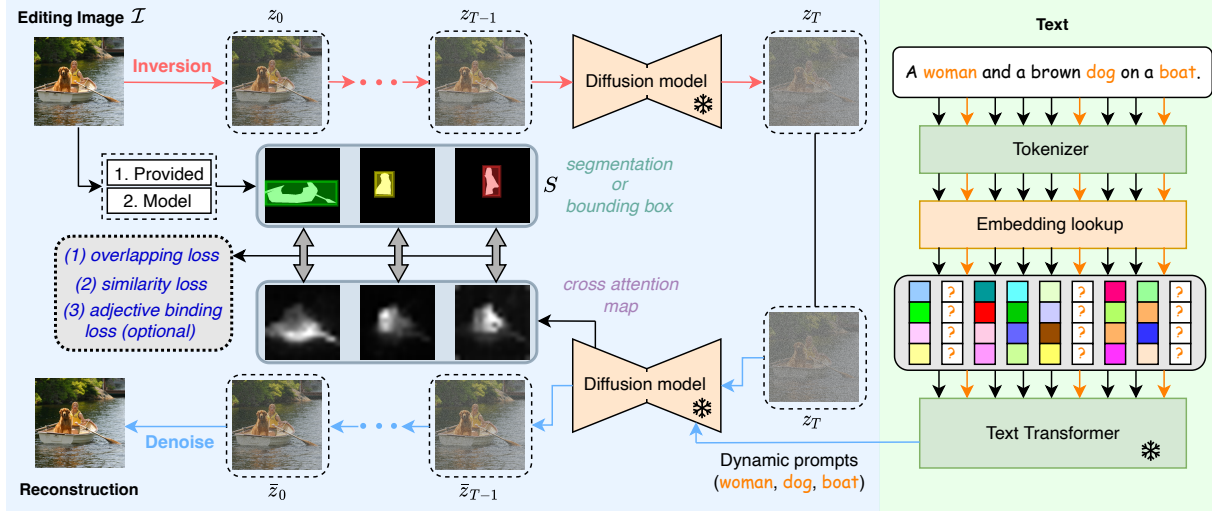


Figure 2. Illustration of our proposed method *LocInv*. The image \mathcal{I} comes with its *localization prior* denoted as S (segmentation maps or detection boxes). For each time stamp t , the noun (and optionally adjective) words in the text prompt are transformed into dynamic tokens, as introduced in Sec 3.2. In each denoising step $\bar{z}_{t-1} \rightarrow \bar{z}_t$, we update the dynamic token set \mathcal{V}_t with our proposed overlapping loss, similarity loss and adjective binding loss, in order to ensure high-quality cross-attention maps.

the most representative prompt-based segmentation model is SAM [27]. Given an image and visual prompt (box, points, text, or mask), SAM encodes image and prompt embeddings using an image and prompt encoder, respectively which are then combined in a lightweight mask decoder that predicts segmentation masks. Similar works include CLIPSeg [32], OpenSeg [14], GroupViT [58], etc. For prompt-based object detector, GroundingDINO [31] stands out as the state-of-the-art method by grounding the DINO [6] detector with language pre-training for open-set generalization. Except that, MaskCLIP [12], X-decoder [64], UniDetector [56] also offer prompt-based detectors. Leveraging these foundational models, we can acquire localization information as a valuable semantic prior to enhance image inversion. This, in turn, contributes to an overall improvement in image editing performance.

3. Methodology

In this section, we provide the description of our method *LocInv*. An illustration of our method is shown in Fig. 2 and the pseudo-code in Algorithm 1.

3.1. Preliminary

Latent Diffusion Models. We use Stable Diffusion v1.4 which is a Latent Diffusion Model (LDM) [45]. The model is composed of two main components: an autoencoder and a diffusion model. The encoder \mathcal{E} from the autoencoder component of the LDMs maps an image \mathcal{I} into a latent code $z_0 = \mathcal{E}(\mathcal{I})$ and the decoder reverses the latent code back to the original image as $\mathcal{D}(\mathcal{E}(\mathcal{I})) \approx \mathcal{I}$. The diffusion model can be conditioned on class labels, segmentation masks or textual input. Let $\tau_\theta(y)$ be the conditioning mech-

anism which maps a condition y into a conditional vector for LDMs, the LDM model is updated by the loss:

$$L_{ldm} = \mathbb{E}_{z_0 \sim \mathcal{E}(x), y, \epsilon \sim \mathcal{N}(0,1)} \left[\|\epsilon - \epsilon_\theta(z_t, t, \tau_\theta(y))\|_2^2 \right] \quad (1)$$

The neural backbone ϵ_θ is typically a conditional UNet [46] which predicts the added noise. More specifically, text-guided diffusion models aim to generate an image from a random noise z_T and a conditional input prompt \mathcal{P} . To distinguish from the general conditional notation in LDMs, we itemize the textual condition as $\mathcal{C} = \tau_\theta(\mathcal{P})$.

DDIM inversion. Inversion aims to find an initial noise z_T reconstructing the input latent code z_0 upon sampling. Since we aim at accurate reconstruction of a given image for image editing, we employ the deterministic DDIM sampler:

$$z_{t+1} = \sqrt{\bar{\alpha}_{t+1}} f_\theta(z_t, t, \mathcal{C}) + \sqrt{1 - \bar{\alpha}_{t+1}} \epsilon_\theta(z_t, t, \mathcal{C}) \quad (2)$$

where $\bar{\alpha}_{t+1}$ is noise scaling factor defined in DDIM [49] and $f_\theta(z_t, t, \mathcal{C})$ predicts the final denoised latent code z_0 as $f_\theta(z_t, t, \mathcal{C}) = \left[z_t - \sqrt{1 - \bar{\alpha}_t} \epsilon_\theta(z_t, t, \mathcal{C}) \right] / \sqrt{\bar{\alpha}_t}$.

Null-Text inversion (NTI). To amplify the effect of conditional textual prompts, classifier-free guidance (CFG) [20] is proposed to extrapolate the conditional noise with an unconditional noise prediction. Let $\emptyset = \tau_\theta(\text{" "})$ denote the *null-text* embedding, the CFG is defined as:

$$\tilde{\epsilon}_\theta(z_t, t, \mathcal{C}, \emptyset) = w \cdot \epsilon_\theta(z_t, t, \mathcal{C}) + (1-w) \cdot \epsilon_\theta(z_t, t, \emptyset) \quad (3)$$

where we set the guidance scale $w = 7.5$ as is standard for LDM [20, 37, 45]. However, the introduction of CFG complicates the inversion, and the generated image from the found initial noise z_T deviates from the input image. NTI [37] proposes a novel optimization which updates the

null text embedding \varnothing_t for each DDIM step $t \in [1, T]$ to approximate the DDIM trajectory $\{z_t\}_0^T$ according to:

$$\min_{\varnothing_t} \|\bar{z}_{t-1} - \tilde{\epsilon}_\theta(\bar{z}_t, t, \mathcal{C}, \varnothing_t)\|_2^2 \quad (4)$$

where $\{\bar{z}_t\}_0^T$ is the backward trace from NTI. This allows to edit real images starting from initial noise $\bar{z}_T = z_T$ using the learned null-text \varnothing_t in combination with P2P [18].

3.2. Dynamic Prompt Learning

Text-based image editing takes an image \mathcal{I} described by an initial prompt \mathcal{P} , and aims to modify it according to an altered prompt \mathcal{P}^* in which the user indicates desired changes. The initial prompt is used to compute the cross-attention maps. As discussed in Sec. 1, *cross-attention leakage* [53] is a challenge for existing text-based editing methods, when facing complex scenarios. DPL [53] introduces three losses to enhance the alignment between attention maps and nouns, which rely on the inherent connection between image and prompt and is not always reliable in real-world scenarios. In this section, we present our method, denoted as *LocInv*, which leverages localization priors derived from existing segmentation maps (*Segment-Prior*) or detection boxes (*Detection-Prior*). This information can be readily acquired with the assistance of recent advancements in foundation models [27, 65] and has the potential to dramatically strengthen the quality of the cross-attention maps. To simplify, we denote the segmentation map and detection boxes uniformly as S .

The cross-attention maps in the Diffusion Model UNet are obtained from $\epsilon_\theta(z_t, t, \mathcal{C})$, which is the first component in Eq. 3. They are computed from the deep features of the noisy image $\psi(z_t)$ which are projected to a query matrix $Q_t = l_Q(\psi(z_t))$, and the textual embedding which is projected to a key matrix $K = l_K(\mathcal{C})$. Then the attention map is computed as $A_t = \text{softmax}(Q_t \cdot K^T / \sqrt{d})$, where d is the latent dimension, and the cell $[A_t]_{ij}$ defines the weight of the j -th token on the pixel i . We optimize the word embeddings v corresponding to the initial prompt \mathcal{P} in such a way that the resulting cross-attention A_t does not suffer from the above-mentioned cross-attention leakage. The initial prompt \mathcal{P} contains K noun words and their corresponding learnable tokens at each timestamp $\mathcal{V}_t = \{v_t^1, \dots, v_t^k, \dots, v_t^K\}$. Similar to DPL, *LocInv* updates each specified word in \mathcal{V}_t for each step t . The final sentence embedding \mathcal{C}_t now varies for each timestamp t and is computed by applying the text encoder on the text embeddings.

3.3. *LocInv*: Localization-aware Inversion

To update the token representations in each timestep, we propose several losses to optimize the embedding vectors \mathcal{V}_t : we develop one loss to address the similarity and another one to ensure high overlapping, between the cross-attention map and its corresponding location prior S .

Similarity loss. The similarity is defined as the cosine distance between the attention map and the location prior.

$$\mathcal{L}_{sim} = \sum_{i=1}^K [1 - \cos(\mathcal{A}_t^{v_t^i}, S_t^{v_t^i})] \quad (5)$$

Nonetheless, our experiments reveal that solely employing the similarity loss leads to lower Intersection over Union (IoU) curves. Given that attention maps are continuous functions, we have additionally introduced an overlapping loss to gently restrict the cross-attention.

Overlapping loss. This loss is defined as the percentage of the attention map locating in the localization prior as:

$$\mathcal{L}_{ovl} = 1 - \frac{\sum_{i=1}^K \mathcal{A}_t^{v_t^i} \cdot S_t^{v_t^i}}{\sum_{i=1}^K \mathcal{A}_t^{v_t^i}} \quad (6)$$

By incorporating both losses, our method effectively aligns the cross-attention maps with the localization priors. We update the learnable token v_t^k according to:

$$\arg \min_{\mathcal{V}_t} \mathcal{L} = \lambda_{sim} \cdot \mathcal{L}_{sim} + \lambda_{ovl} \cdot \mathcal{L}_{ovl} \quad (7)$$

Gradual Optimization for Token Updates. So far, we introduced the losses to learn new dynamic tokens at each timestamp. However, the cross-attention leakage gradually accumulated in the denoising phase. Hence, we enforce all losses to reach a pre-defined threshold at each timestamp t to avoid overfitting the cross-attention maps [53]. We express the gradual threshold by an exponential function. For the losses proposed above, the corresponding thresholds at time t are defined as $TH_t = \beta \cdot \exp(-t/\alpha)$. And for each loss we have a group of hyperparameters as $(\beta_{sim}, \alpha_{sim}), (\beta_{ovl}, \alpha_{ovl}), (\beta_{adj}, \alpha_{adj})$. We verify the effectiveness of this mechanism in our ablation experiments.

Null-Text embeddings. The above described token updating ensures that the cross-attention maps are highly related to the noun words in the text prompt and minimize cross-attention leakage. To reconstruct the original image, we use NTI [37] in addition to learn a set of null embeddings \varnothing_t for each timestamp t . Then we have a set of learnable word embeddings \mathcal{V}_t and null text \varnothing_t which can accurately localize the objects and also reconstruct the original image.

3.4. Adjective binding

Existing text-guided image editing methods have focused on translating a source object to a target one. However, often users would like to change the appearance of objects. Typically, in text-guided image editing, this would be done by changing the objects' attributes described by adjectives. However, existing methods fail when editing attributes of the source objects (as shown in Fig. 5). We ascribe this case

Algorithm 1: Localization-aware Inversion

- 1 **Input:** A source prompt \mathcal{P} , an input image \mathcal{I} , the localization prior $S, T = 50$
 - 2 **Output:** A noise vector \bar{z}_T , a set of updated tokens $\{\mathcal{V}_t\}_1^T$ and null-text embeddings $\{\varnothing_t\}_1^T$
 - 3 $\{z_t\}_0^T \leftarrow \text{DDIM-inv}(\mathcal{I});$
 - 4 Set guidance scale $w = 7.5;$
 - 5 Initialize \mathcal{V}_T with original noun tokens;
 - 6 Initialize $\bar{z}_T = z_T, \mathcal{P}_T = \mathcal{P}, \varnothing_T = \tau_\theta(\text{""});$
 - 7 **for** $t = T, T - 1, \dots, 1$ **do**
 - 8 Initialize \mathcal{P}_t by \mathcal{V}_t , then $\mathcal{C}_t = \tau_\theta(\mathcal{P}_t);$
 - 9 Compute $\mathcal{L}_{sim}, \mathcal{L}_{ovl}, \mathcal{L}_{adj}$ by Eq.5-8;
 - 10 **while** $\mathcal{L}_{sim} \geq TH_t^{sim}$ **or** $\mathcal{L}_{ovl} \geq TH_t^{ovl}$ **or**
 $\mathcal{L}_{adj} \geq TH_t^{adj}$ **do**
 - 11 $\mathcal{L} = \lambda_{sim} \cdot \mathcal{L}_{sim} + \lambda_{ovl} \cdot \mathcal{L}_{ovl} + \lambda_{adj} \cdot \mathcal{L}_{adj}$
 - 12 $\mathcal{V}_t \leftarrow \mathcal{V}_t - \nabla_{\mathcal{V}_t} \mathcal{L}$
 - 13 **end**
 - 14 $\bar{z}_t = \tilde{\epsilon}_\theta(\bar{z}_t, t, \mathcal{C}_t, \varnothing_t)$
 - 15 $\bar{z}_{t-1}, \varnothing_t \leftarrow NTI(\bar{z}_t, \varnothing_t)$
 - 16 Initialize $\varnothing_{t-1} \leftarrow \varnothing_t, \mathcal{V}_{t-1} \leftarrow \mathcal{V}_t$
 - 17 **end**
 - 18 **Return** $\bar{z}_T, \{\mathcal{V}_t\}_1^T, \{\varnothing_t\}_1^T$
-

to the disagreement in cross-attention between the adjective and its corresponding noun word (as evidenced in Fig. 1).

To empower the T2I model with attribute editing capability, we propose to bind the adjective words with their corresponding nouns. To achieve this, we use the Spacy parser [22] to detect the object noun and adjective words, as so called the adjective-noun pairs (v_t^i, a_t^i) . Given these pairs, the adjective binding loss is defined as the similarity between the attention maps of the adjective and noun words.

$$\mathcal{L}_{adj} = \sum_{i=1}^K [1 - \cos(\mathcal{A}_t^{v_t^i}, \mathcal{A}_t^{a_t^i})] \quad (8)$$

This loss ensures maximum overlap between the adjective-noun pairs and is only applied when Adjective-Edit is demanded, and we simply add $\lambda_{adj} \cdot \mathcal{L}_{adj}$ to Eq. 7.

4. Experiments

We demonstrate *LocInv* in various experiments based on the open-source Stable Diffusion [45] following previous methods [37, 39, 52]. All experiments are done on R6000 GPUs.

Datasets. For the quantitative ablation study of hyperparameters and partially for the qualitative editing comparison, we select 315 images as a subset *COCO-edit* out of MS-COCO dataset [30]. We compose this subset from various searching prompts (including concepts as airplane, apple, banana, bear, bench, etc.) and store the groundtruth seg-

User Study (%)						
method	LocInv (Seg)	DiffEdit	MasaCtrl	NTI	pix2pix	PnP
Edit quality	40.0	27.0	3.5	25.5	0.75	3.25
Background	25.8	3.7	4.5	20.0	22.7	23.3

Table 1. User study compared with methods freezing the Stable Diffusion [45]. We request the respondents to evaluate methods in both editing quality and background preservations.

mentation/detection images for experimental usage. Overall, there are 7 search prompts with a single object (noun) in the sentence and 6 with multiple objects. More detailed information is shown in the supplementary material.

Compared methods. We organize two groups of methods for qualitative and quantitative comparison. The first group of methods, which are *freezing* the Stable Diffusion models, include NTI [37], DPL [53], pix2pix-zero [39], PnP [52], DiffEdit [11] and MasaCtrl [5]. The second group of methods is *finetuning* the large pretrained T2I model as specific models for image editing, such as SD-inpaint [45], Instruct-Pix2Pix [4] and Imagic [25], or taking *masks* as locations for *inpainting*, including SD-inpaint [45] and BLD [2].

Evaluation metrics. To quantitatively assess our method’s performance, we employ well-established metrics, including LPIPS [61], SSIM [55], PSNR, CLIP-Score [19] and DINO-Sim [51], to evaluate the edited full image. Additionally, to illustrate the quality of background preservation, we follow DirectInversion [24] to compute LPIPS, SSIM, PSNR, and MSE metrics for regions outside the mask.

4.1. Ablation study

For the ablation study, we experiment on the *COCO-edit* dataset. To quantitatively assess the localization performance of *LocInv*, we vary the threshold from 0.0 to 1.0 to obtain the segmentation mask from the cross-attention maps. We then calculated the Intersection over Union (IoU) metric using the segmentation ground truth for comparison. Our method can operate with both segmentation maps and detection bounding boxes as localization priors. Here, we consider the hyperparameters for both these cases.

In Fig. 3, we conduct ablation studies over the similarity loss and the overlapping loss. From Fig. 3-(c)(g), we observe that only applying one of these losses does not ensure a satisfactory performance. Empirically, we find the optimal hyperparameters for the segmentation and detection prior as $\lambda_{sim} = 1.0, \alpha_{sim} = 50.0, \beta_{sim} = 0.7, \lambda_{ovl} = 1.0, \alpha_{ovl} = 10.0, \beta_{ovl} = 0.7$ and $\lambda_{sim} = 0.1, \alpha_{sim} = 25.0, \beta_{sim} = 0.5, \lambda_{ovl} = 1.0, \alpha_{ovl} = 25.0, \beta_{ovl} = 0.3$, respectively. For the adjective binding loss, since there are no sufficient image-text pairs for the ablation study, we empirically set the hyperparameters to be $\lambda_{adj} = 2.0, \alpha_{adj} = 50.0, \beta_{adj} = 0.1$. All results in this paper are generated with this hyperparameter setting.

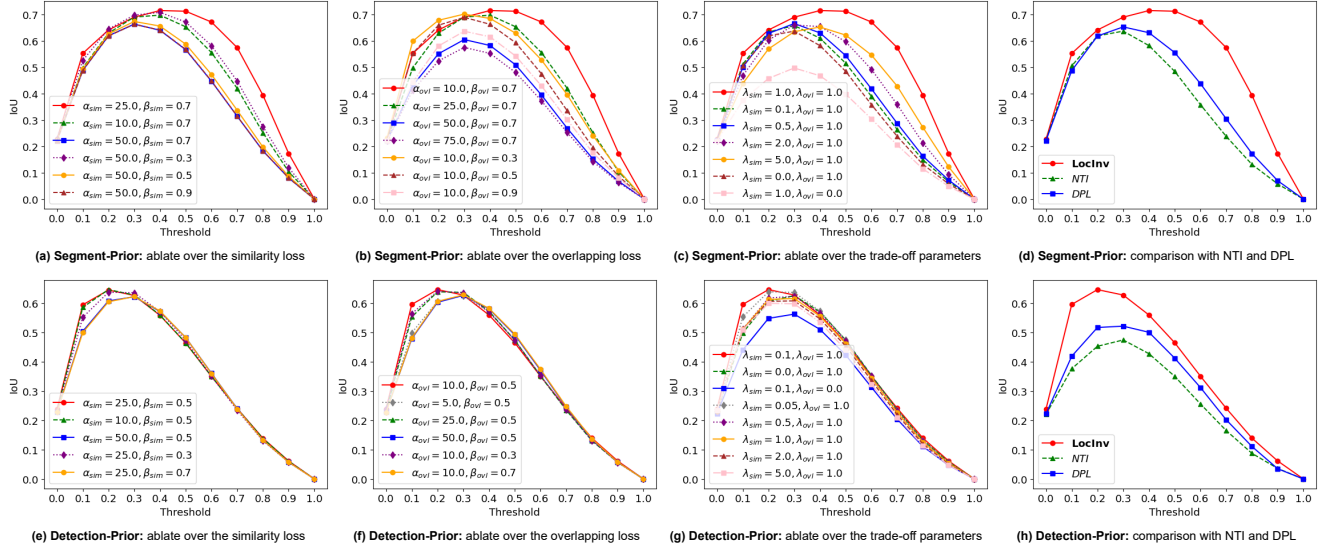


Figure 3. Ablation study over hyperparameters given the Segment-Prior (first row) or Detection-Prior (second row). For the first and second columns, we ablate hyperparameters for the similarity loss and overlapping loss, respectively. Then we illustrate how the trade-off parameters influence in the third column. Lastly, we show the IoU curves of *LoClnv* together with NTI and DPL as baseline comparisons.

Method	Full Image Evaluation				Background Preservation				CLIP-Score(↑)	
	LPIPS(↓)	SSIM(↑)	PSNR(↑)	DINO-Sim(↓)	MSE(↓)	LPIPS(↓)	SSIM(↑)	PSNR(↑)	Edited	Original
Multi-Object Image Editing (6 tasks)										
Freezing SD	DiffEdit [11]	0.2821	0.5910	18.5804	<u>0.0219</u>	0.0066	0.1981	0.6888	22.7726	21.4439
	pix2pix [39]	0.4047	0.5492	19.7397	0.0549	0.0152	0.3347	0.6262	20.9542	21.8384
	NTI [37]	0.2936	0.5919	<u>21.7963</u>	0.0433	0.0118	0.2413	0.6644	23.1352	21.7216
	DPL [53]	<u>0.2686</u>	0.6121	21.3193	0.0223	0.0071	0.2299	0.6601	22.2695	21.5982
	PnP [52]	0.3960	0.5568	18.8198	0.0384	0.0113	0.3331	0.6243	19.8573	<u>21.8470</u>
	MasaCtrl [5]	0.4406	0.4671	17.3948	0.0611	0.0198	0.3784	0.5309	18.2041	21.7835
	<i>LoClnv</i> (Det)	0.2935	0.5956	21.3116	0.0272	0.0065	0.2458	0.6532	22.5126	21.6615
<i>LoClnv</i> (Seg)	0.2523	<u>0.6161</u>	22.3027	0.0181	<u>0.0054</u>	0.1970	0.6905	24.3783	21.7757	
Finetuning SD	Imagic [25]	0.7347	0.2098	9.9586	0.1217	0.0935	0.6166	0.3280	10.7490	21.7566
	InstructP2P [4]	0.3330	0.5428	17.4007	0.0274	0.0150	0.2462	0.6407	20.2072	21.6666
	Inpaint (Det) [45]	0.3710	0.4853	16.9441	0.1242	0.0398	0.2755	0.6075	21.5161	21.8475
	Inpaint (Seg) [45]	0.2703	0.6040	19.2707	0.0299	0.0061	0.1620	<u>0.7233</u>	<u>26.3149</u>	21.8315
	BLD (Det) [2]	0.3412	0.5604	17.0294	0.0405	0.0112	0.2424	0.6814	21.0436	21.7218
	BLD (Seg) [2]	0.2924	0.6257	18.9036	0.0258	0.0031	<u>0.1845</u>	0.7426	26.5964	21.7806
	Single-Object Image Editing (7 tasks)									
Freezing SD	DiffEdit [11]	0.2990	0.5701	17.7486	0.0278	0.0057	0.1873	0.7136	23.4800	21.4608
	pix2pix [39]	0.4398	0.4824	17.2601	0.0645	0.0171	0.3180	0.6332	20.1122	<u>21.8336</u>
	NTI [37]	0.2758	0.5864	21.4369	0.0280	0.0092	0.1936	0.7001	24.3014	21.7665
	DPL [53]	<u>0.2743</u>	<u>0.5906</u>	21.1188	0.0212	0.0061	0.1791	0.7133	25.1545	21.7944
	PnP [52]	0.3983	0.5379	18.0061	0.0338	0.0111	0.2893	0.6688	20.0125	21.7214
	MasaCtrl [5]	0.4004	0.4472	17.2875	0.0430	0.0138	0.2879	0.5957	19.4637	22.0493
	<i>LoClnv</i> (Det)	0.2756	0.5867	21.1920	<u>0.0196</u>	0.0049	0.1810	0.7118	25.1956	21.7308
<i>LoClnv</i> (Seg)	0.2662	0.5952	<u>21.2287</u>	0.0180	0.0047	0.1730	0.7193	25.2118	21.8069	
Finetuning SD	Imagic [25]	0.6657	0.2429	10.8554	0.1418	0.0694	0.5107	0.4313	12.3759	21.8340
	InstructP2P [4]	0.3684	0.4925	16.3615	0.0421	0.0177	0.2519	0.6477	19.7768	21.7257
	Inpaint (Det) [45]	0.3034	0.5458	17.4352	0.0301	<u>0.0039</u>	0.1570	<u>0.7300</u>	<u>26.4033</u>	21.7324
	Inpaint (Seg) [45]	0.3080	0.5380	17.3868	0.0304	0.0038	<u>0.1599</u>	0.7241	26.4464	21.7967
	BLD (Det) [2]	0.4112	0.4729	15.3787	0.0861	0.0175	0.2676	0.6649	18.9651	21.6654
	BLD (Seg) [2]	0.3423	0.5571	17.4153	0.0455	0.0040	0.1895	0.7478	25.6214	21.6880

Table 2. Comparison with various text-based image editing methods based on the evaluation metrics over the *COCO-edit* dataset. We evaluate on single-object and multi-object images editing tasks separately. The comparison methods are organized into two groups as we stated in Sec. 4 The “Seg” and “Det” in the bracket represent the Segment-prior and Detection-Prior, respectively.

Caption	an <apple> a <banana> a cup of orange juice	A ripe <banana> with a red <apple> sitting on a wood table	a white <cat> a wooden <bench> and some pumpkins	A <cat> sitting on a wooden <bench> outside in a garden area	A brown <bear> walking across a forest surrounded by trees	a <zebra> standing on some dirt and bushes and trees	A little <dog> is smiling yet panting with a <frisbee> at his side	there is a <dog> and a <cat> sitting in a basket	a <dog> and a <cat> laying beside each other on a lonely street
	apple → peach	apple → tomato	cat → tiger	cat → cougar	bear → panda	zebra → horse	dog → cat	dog → cat	dog → wolf
Input									
Ours									
NIT									
DiffEdit									
pix2pix-zero									
MaskCurl									
PaP									
BLD									
Imagic									
Instruct2P									
SD-inpaint									

Freezing Stable Diffusion

Finetuning Stable Diffusion

Figure 4. Comparison over the local object Word-Swap editing given the *Segment-Prior*. All examples are from the COCO-edit dataset. We distinguish these comparison methods by (1) freezing the SD [45] models; (2) fine-tuning the SD models or mask-based inpainting.

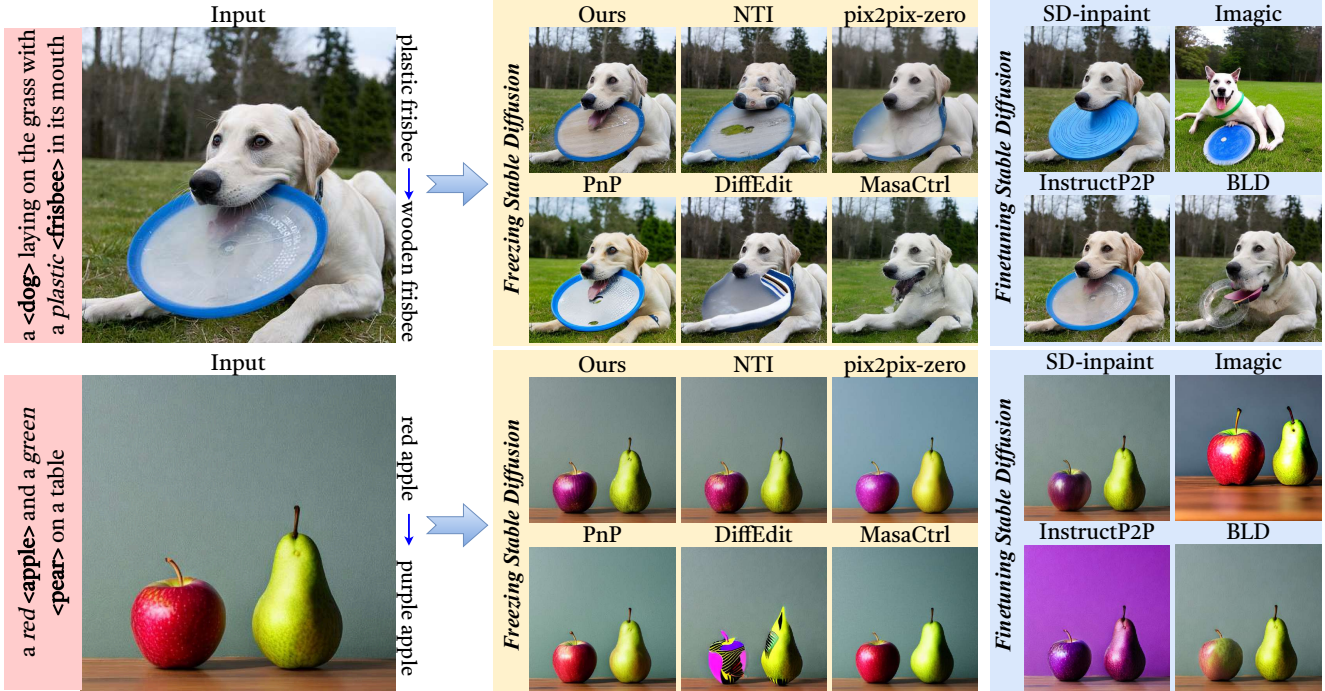


Figure 5. Attribute-Edit by swapping the adjectives given the *Segment-Prior*. By forcing the binding between the cross-attention from the adjective words and corresponding noun words, *LoCInv* successfully edits the color or material attribute.

4.2. Image editing evaluation

For image editing, we combine *LoCInv* with the P2P [18] image editing method. In this paper, we mainly focus on local editing tasks including Word-Swap and Attribute-Edit.

Word-Swap. As shown in Fig. 4, we compare *LoCInv* with various methods by swapping one object from the original image given the segmentation maps as localization priors. Our method, *LoCInv*, more successfully translates the source object into the target object while maintaining semantic similarities. In Table 2, we designed one editing task for each group of images collected in the COCO-Edit dataset (details in the supplementary material). In both single-object and multi-object editing tasks, *LoCInv* achieves better full image evaluation and only performs worse than the inpainting-based methods [2, 45] in terms of background preservation (since these methods do not change background pixels). It is worth noting that *LoCInv* does not require fine-tuning the base model, resulting in better time complexity and no forgetting in the T2I models. In Table 1, we question twenty participants to evaluate the image editing performance from two aspects: the editing quality and the background preservation. In both cases, *LoCInv* stands out of these six methods of freezing the SD models. Details on the user study are shown in the supplementary.

Attribute-Edit. Furthermore, *LoCInv* excels in another editing aspect that other methods tend to overlook, which is attribute editing. This capability is illustrated in Fig. 5.

By force the binding between the adjective words and their corresponding noun objects, we achieve the capacity to accurately modify their attributes (color, material, etc.).

5. Conclusion

In this paper, we presented *Localization-aware Inversion (LoCInv)* to solve the cross-attention leakage problem in image editing using text-to-image diffusion models. We propose to update the dynamic tokens for each noun word in the prompt with the segmentation or detection as the prior. The resulting cross-attention maps suffer less from cross-attention leakage. Consequently, these greatly improved cross-attention maps result in considerably better results for text-guided image editing. The experimental results, confirm that *LoCInv* obtains superior results, especially on complex multi-object scenes. Finally, we show that our method can also bind the adjective words to their corresponding nouns, leading to accurate cross-attention maps for the adjectives, and allowing for attribute editing which has not been well explored before for text-guided image editing.

Acknowledgments We acknowledge projects TED2021-132513B-I00 and PID2022-143257NB-I00, financed by MCIN/AEI/10.13039/501100011033 and FSE+ by the European Union NextGenerationEU/PRTR, and by ERDF A Way of Making Europa, and the Generalitat de Catalunya CERCA Program. Chuanming Tang acknowledges the Chinese Scholarship Council (CSC) No.202204910331.

References

- [1] Omri Avrahami, Dani Lischinski, and Ohad Fried. Blended diffusion for text-driven editing of natural images. In *Proceedings of the IEEE/CVF Conference on Computer Vision and Pattern Recognition*, pages 18208–18218, 2022. [2](#)
- [2] Omri Avrahami, Ohad Fried, and Dani Lischinski. Blended latent diffusion. *ACM Transactions on Graphics (TOG)*, 42(4):1–11, 2023. [2](#), [5](#), [6](#), [8](#)
- [3] Omer Bar-Tal, Dolev Ofri-Amar, Rafail Fridman, Yoni Kasten, and Tali Dekel. Text2live: Text-driven layered image and video editing. In *European Conference on Computer Vision*, pages 707–723. Springer, 2022. [2](#)
- [4] Tim Brooks, Aleksander Holynski, and Alexei A. Efros. Instructpix2pix: Learning to follow image editing instructions. In *Proceedings of the IEEE Conference on Computer Vision and Pattern Recognition*, 2023. [2](#), [5](#), [6](#), [12](#)
- [5] Mingdeng Cao, Xintao Wang, Zhongang Qi, Ying Shan, Xiaohu Qie, and Yinqiang Zheng. Masactrl: Tuning-free mutual self-attention control for consistent image synthesis and editing. *Proceedings of the International Conference on Computer Vision*, 2023. [5](#), [6](#), [13](#)
- [6] Mathilde Caron, Hugo Touvron, Ishan Misra, Hervé Jégou, Julien Mairal, Piotr Bojanowski, and Armand Joulin. Emerging properties in self-supervised vision transformers. In *Proceedings of the IEEE/CVF international conference on computer vision*, pages 9650–9660, 2021. [3](#)
- [7] Huiwen Chang, Han Zhang, Jarred Barber, AJ Maschinot, Jose Lezama, Lu Jiang, Ming-Hsuan Yang, Kevin Murphy, William T Freeman, Michael Rubinstein, et al. Muse: Text-to-image generation via masked generative transformers. *International Conference on Machine Learning*, 2023. [2](#)
- [8] Songyan Chen and Jiancheng Huang. Fec: Three finetuning-free methods to enhance consistency for real image editing. *arXiv preprint arXiv:2309.14934*, 2023. [1](#)
- [9] Shoufa Chen, Peize Sun, Yibing Song, and Ping Luo. Diffusiondet: Diffusion model for object detection. *arXiv preprint arXiv:2211.09788*, 2022. [12](#)
- [10] Jooyoung Choi, Sungwon Kim, Yonghyun Jeong, Youngjune Gwon, and Sungroh Yoon. Ilvr: Conditioning method for denoising diffusion probabilistic models. In *Proceedings of the International Conference on Computer Vision*, pages 14347–14356. IEEE, 2021. [2](#)
- [11] Guillaume Couairon, Jakob Verbeek, Holger Schwenk, and Matthieu Cord. Diffedit: Diffusion-based semantic image editing with mask guidance. In *The Eleventh International Conference on Learning Representations*, 2023. [2](#), [5](#), [6](#), [13](#)
- [12] Zheng Ding, Jieke Wang, and Zhuowen Tu. Open-vocabulary panoptic segmentation with maskclip. *International Conference on Machine Learning*, 2023. [3](#)
- [13] Oran Gafni, Adam Polyak, Oron Ashual, Shelly Sheynin, Devi Parikh, and Yaniv Taigman. Make-a-scene: Scene-based text-to-image generation with human priors. In *European Conference on Computer Vision*, pages 89–106. Springer, 2022. [2](#)
- [14] Golnaz Ghiasi, Xiuye Gu, Yin Cui, and Tsung-Yi Lin. Scaling open-vocabulary image segmentation with image-level labels. In *European Conference on Computer Vision*, pages 540–557. Springer, 2022. [3](#)
- [15] Asya Grechka, Guillaume Couairon, and Matthieu Cord. Gradpaint: Gradient-guided inpainting with diffusion models. *arXiv preprint arXiv:2309.09614*, 2023. [2](#)
- [16] Ligong Han, Song Wen, Qi Chen, Zhixing Zhang, Kunpeng Song, Mengwei Ren, Ruijiang Gao, Yuxiao Chen, Di Liu, Qilong Zhangli, et al. Improving negative-prompt inversion via proximal guidance. *arXiv preprint arXiv:2306.05414*, 2023. [2](#)
- [17] Amir Hertz, Kfir Aberman, and Daniel Cohen-Or. Delta denoising score. *arXiv preprint arXiv:2304.07090*, 2023. [1](#)
- [18] Amir Hertz, Ron Mokady, Jay Tenenbaum, Kfir Aberman, Yael Pritch, and Daniel Cohen-Or. Prompt-to-prompt image editing with cross attention control. *International Conference on Learning Representations*, 2023. [2](#), [4](#), [8](#)
- [19] Jack Hessel, Ari Holtzman, Maxwell Forbes, Ronan Le Bras, and Yejin Choi. Clipscore: A reference-free evaluation metric for image captioning. In *Proceedings of the 2021 Conference on Empirical Methods in Natural Language Processing*, pages 7514–7528, 2021. [5](#)
- [20] Jonathan Ho and Tim Salimans. Classifier-free diffusion guidance. *NeurIPS 2021 Workshop on Deep Generative Models and Downstream Applications*, 2022. [2](#), [3](#)
- [21] Susung Hong, Gyuseong Lee, Wooseok Jang, and Seungryong Kim. Improving sample quality of diffusion models using self-attention guidance. *Proceedings of the International Conference on Computer Vision*, 2023. [2](#)
- [22] Matthew Honnibal and Ines Montani. spacy 2: Natural language understanding with bloom embeddings, convolutional neural networks and incremental parsing. *To appear*, 7(1): 411–420, 2017. [5](#)
- [23] Jiancheng Huang, Yifan Liu, Jin Qin, and Shifeng Chen. Kv inversion: Kv embeddings learning for text-conditioned real image action editing. *arXiv preprint arXiv:2309.16608*, 2023. [2](#)
- [24] Xuan Ju, Ailing Zeng, Yuxuan Bian, Shaoteng Liu, and Qiang Xu. Direct inversion: Boosting diffusion-based editing with 3 lines of code. *arXiv preprint arXiv:2310.01506*, 2023. [2](#), [5](#)
- [25] Bahjat Kawar, Shiran Zada, Oran Lang, Omer Tov, Huiwen Chang, Tali Dekel, Inbar Mosseri, and Michal Irani. Imagic: Text-based real image editing with diffusion models. *Proceedings of the IEEE Conference on Computer Vision and Pattern Recognition*, 2023. [2](#), [5](#), [6](#)
- [26] Gwanghyun Kim, Taesung Kwon, and Jong Chul Ye. Diffusionclip: Text-guided diffusion models for robust image manipulation. In *Proceedings of the IEEE/CVF Conference on Computer Vision and Pattern Recognition (CVPR)*, pages 2426–2435, 2022. [2](#)
- [27] Alexander Kirillov, Eric Mintun, Nikhila Ravi, Hanzi Mao, Chloe Rolland, Laura Gustafson, Tete Xiao, Spencer Whitehead, Alexander C. Berg, Wan-Yen Lo, Piotr Dollár, and Ross Girshick. Segment anything. *Proceedings of the International Conference on Computer Vision*, 2023. [1](#), [3](#), [4](#)
- [28] Gihyun Kwon and Jong Chul Ye. Diffusion-based image translation using disentangled style and content representa-

- tion. In *The Eleventh International Conference on Learning Representations*, 2023. [2](#)
- [29] Senmao Li, Joost van de Weijer, Taihang Hu, Fahad Shahbaz Khan, Qibin Hou, Yaxing Wang, and Jian Yang. Stylediffusion: Prompt-embedding inversion for text-based editing, 2023. [1](#), [2](#)
- [30] Tsung-Yi Lin, Michael Maire, Serge Belongie, James Hays, Pietro Perona, Deva Ramanan, Piotr Dollár, and C Lawrence Zitnick. Microsoft coco: Common objects in context. In *European Conference on Computer Vision*, pages 740–755. Springer, 2014. [2](#), [5](#)
- [31] Shilong Liu, Zhaoyang Zeng, Tianhe Ren, Feng Li, Hao Zhang, Jie Yang, Chunyuan Li, Jianwei Yang, Hang Su, Jun Zhu, and Lei Zhang. Grounding dino: Marrying dino with grounded pre-training for open-set object detection. In *arXiv preprint arXiv:2303.05499*, 2023. [1](#), [3](#)
- [32] Timo Lüddecke and Alexander Ecker. Image segmentation using text and image prompts. In *Proceedings of the IEEE/CVF Conference on Computer Vision and Pattern Recognition*, pages 7086–7096, 2022. [3](#)
- [33] Andreas Lugmayr, Martin Danelljan, Andres Romero, Fisher Yu, Radu Timofte, and Luc Van Gool. Repaint: Inpainting using denoising diffusion probabilistic models. In *Proceedings of the IEEE/CVF Conference on Computer Vision and Pattern Recognition*, pages 11461–11471, 2022. [2](#)
- [34] Chenlin Meng, Yutong He, Yang Song, Jiaming Song, Jiajun Wu, Jun-Yan Zhu, and Stefano Ermon. SDEdit: Guided image synthesis and editing with stochastic differential equations. In *International Conference on Learning Representations*, 2022. [2](#)
- [35] Midjourney.com. Midjourney. <https://www.midjourney.com>, 2022. [1](#)
- [36] Daiki Miyake, Akihiro Iohara, Yu Saito, and Toshiyuki Tanaka. Negative-prompt inversion: Fast image inversion for editing with text-guided diffusion models. *arXiv preprint arXiv:2305.16807*, 2023. [2](#)
- [37] Ron Mokady, Amir Hertz, Kfir Aberman, Yael Pritch, and Daniel Cohen-Or. Null-text inversion for editing real images using guided diffusion models. *Proceedings of the IEEE Conference on Computer Vision and Pattern Recognition*, 2023. [1](#), [2](#), [3](#), [4](#), [5](#), [6](#), [12](#), [13](#), [14](#), [15](#)
- [38] Alexander Quinn Nichol, Prafulla Dhariwal, Aditya Ramesh, Pranav Shyam, Pamela Mishkin, Bob McGrew, Ilya Sutskever, and Mark Chen. GLIDE: Towards photorealistic image generation and editing with text-guided diffusion models. In *Proceedings of the 39th International Conference on Machine Learning*, pages 16784–16804. PMLR, 2022. [2](#)
- [39] Gaurav Parmar, Krishna Kumar Singh, Richard Zhang, Yijun Li, Jingwan Lu, and Jun-Yan Zhu. Zero-shot image-to-image translation. *Proceedings of the ACM SIGGRAPH Conference on Computer Graphics*, 2023. [1](#), [2](#), [5](#), [6](#), [13](#)
- [40] Or Patashnik, Daniel Garibi, Idan Azuri, Hadar Averbuch-Elor, and Daniel Cohen-Or. Localizing object-level shape variations with text-to-image diffusion models. *Proceedings of the International Conference on Computer Vision*, 2023. [2](#)
- [41] Koutilya Pnvr, Bharat Singh, Pallabi Ghosh, Behjat Siddique, and David Jacobs. Ld-znet: A latent diffusion approach for text-based image segmentation. In *Proceedings of the IEEE/CVF International Conference on Computer Vision*, pages 4157–4168, 2023. [12](#)
- [42] Dustin Podell, Zion English, Kyle Lacey, Andreas Blattmann, Tim Dockhorn, Jonas Müller, Joe Penna, and Robin Rombach. Sdxl: improving latent diffusion models for high-resolution image synthesis. *arXiv preprint arXiv:2307.01952*, 2023. [1](#)
- [43] Aditya Ramesh, Mikhail Pavlov, Gabriel Goh, Scott Gray, Chelsea Voss, Alec Radford, Mark Chen, and Ilya Sutskever. Zero-shot text-to-image generation. In *International Conference on Machine Learning*, pages 8821–8831. PMLR, 2021. [2](#)
- [44] Aditya Ramesh, Prafulla Dhariwal, Alex Nichol, Casey Chu, and Mark Chen. Hierarchical text-conditional image generation with clip latents. *arXiv preprint arXiv:2204.06125*, 2022. [2](#)
- [45] Robin Rombach, Andreas Blattmann, Dominik Lorenz, Patrick Esser, and Björn Ommer. High-resolution image synthesis with latent diffusion models. In *Proceedings of the IEEE/CVF Conference on Computer Vision and Pattern Recognition (CVPR)*, pages 10684–10695, 2022. [2](#), [3](#), [5](#), [6](#), [7](#), [8](#), [12](#)
- [46] Olaf Ronneberger, Philipp Fischer, and Thomas Brox. U-net: Convolutional networks for biomedical image segmentation. In *Medical Image Computing and Computer-Assisted Intervention—MICCAI 2015: 18th International Conference, Munich, Germany, October 5-9, 2015, Proceedings, Part III 18*, pages 234–241. Springer, 2015. [3](#)
- [47] Chitwan Saharia, William Chan, Saurabh Saxena, Lala Li, Jay Whang, Emily Denton, Seyed Kamyar Seyed Ghasemipour, Burcu Karagol Ayan, S Sara Mahdavi, Rapha Gontijo Lopes, et al. Photorealistic text-to-image diffusion models with deep language understanding. *Advances in Neural Information Processing Systems*, 2022. [1](#), [2](#)
- [48] Alex Shonenkov, Misha Konstantinov, Daria Bakshandaeva, Christoph Schuhmann, Ksenia Ivanova, and Nadiia Klokova. Deepfloyd-if. <https://github.com/deep-floyd/IF>, 2023. [1](#), [2](#)
- [49] Jiaming Song, Chenlin Meng, and Stefano Ermon. Denoising diffusion implicit models. In *International Conference on Learning Representations*, 2021. [1](#), [2](#), [3](#), [12](#), [14](#), [15](#)
- [50] Chuanming Tang, Kai Wang, and Joost van de Weijer. Iterinv: Iterative inversion for pixel-level t2i models. *Neurips 2023 workshop on Diffusion Models*, 2023. [2](#)
- [51] Narek Tumanyan, Omer Bar-Tal, Shai Bagon, and Tali Dekel. Splicing vit features for semantic appearance transfer. In *Proceedings of the IEEE/CVF Conference on Computer Vision and Pattern Recognition*, pages 10748–10757, 2022. [5](#)
- [52] Narek Tumanyan, Michal Geyer, Shai Bagon, and Tali Dekel. Plug-and-play diffusion features for text-driven image-to-image translation. *Proceedings of the IEEE Conference on Computer Vision and Pattern Recognition*, 2023. [1](#), [2](#), [5](#), [6](#), [13](#)

- [53] Kai Wang, Fei Yang, Shiqi Yang, Muhammad Atif Butt, and Joost van de Weijer. Dynamic prompt learning: Addressing cross-attention leakage for text-based image editing. *Advances in Neural Information Processing Systems*, 2023. [1](#), [2](#), [4](#), [5](#), [6](#), [12](#), [14](#), [15](#)
- [54] Qian Wang, Biao Zhang, Michael Birsak, and Peter Wonka. Mdp: A generalized framework for text-guided image editing by manipulating the diffusion path, 2023. [1](#)
- [55] Zhou Wang, Eero P Simoncelli, and Alan C Bovik. Multiscale structural similarity for image quality assessment. In *The Thirty-Seventh Asilomar Conference on Signals, Systems & Computers, 2003*, pages 1398–1402. Ieee, 2003. [5](#)
- [56] Zhenyu Wang, Yali Li, Xi Chen, Ser-Nam Lim, Antonio Torralba, Hengshuang Zhao, and Shengjin Wang. Detecting everything in the open world: Towards universal object detection. In *Proceedings of the IEEE/CVF Conference on Computer Vision and Pattern Recognition*, pages 11433–11443, 2023. [3](#)
- [57] Tao Wu, Kai Wang, Chuanming Tang, and Jianlin Zhang. Diffusion-based network for unsupervised landmark detection. *Knowledge-Based Systems*, page 111627, 2024. [12](#)
- [58] Jiarui Xu, Shalini De Mello, Sifei Liu, Wonmin Byeon, Thomas Breuel, Jan Kautz, and Xiaolong Wang. Groupvit: Semantic segmentation emerges from text supervision. In *Proceedings of the IEEE/CVF Conference on Computer Vision and Pattern Recognition*, pages 18134–18144, 2022. [1](#), [3](#)
- [59] Jiarui Xu, Sifei Liu, Arash Vahdat, Wonmin Byeon, Xiaolong Wang, and Shalini De Mello. Open-vocabulary panoptic segmentation with text-to-image diffusion models. In *Proceedings of the IEEE/CVF Conference on Computer Vision and Pattern Recognition*, pages 2955–2966, 2023. [12](#)
- [60] Tao Yu, Runseng Feng, Ruoyu Feng, Jinming Liu, Xin Jin, Wenjun Zeng, and Zhibo Chen. Inpaint anything: Segment anything meets image inpainting. *arXiv preprint arXiv:2304.06790*, 2023. [1](#)
- [61] Richard Zhang, Phillip Isola, Alexei A Efros, Eli Shechtman, and Oliver Wang. The unreasonable effectiveness of deep features as a perceptual metric. In *Proceedings of the IEEE conference on computer vision and pattern recognition*, pages 586–595, 2018. [5](#)
- [62] Shiwen Zhang, Shuai Xiao, and Weilin Huang. Forgedit: Text guided image editing via learning and forgetting. *arXiv preprint arXiv:2309.10556*, 2023. [1](#)
- [63] Yufan Zhou, Bingchen Liu, Yizhe Zhu, Xiao Yang, Changyou Chen, and Jinhui Xu. Shifted diffusion for text-to-image generation. In *Proceedings of the IEEE/CVF Conference on Computer Vision and Pattern Recognition*, pages 10157–10166, 2023. [1](#)
- [64] Xueyan Zou, Zi-Yi Dou, Jianwei Yang, Zhe Gan, Linjie Li, Chunyuan Li, Xiyang Dai, Harkirat Behl, Jianfeng Wang, Lu Yuan, et al. Generalized decoding for pixel, image, and language. In *Proceedings of the IEEE/CVF Conference on Computer Vision and Pattern Recognition*, pages 15116–15127, 2023. [3](#)
- [65] Xueyan Zou, Jianwei Yang, Hao Zhang, Feng Li, Linjie Li, Jianfeng Gao, and Yong Jae Lee. Segment everything every-

where all at once. *Advances in Neural Information Processing Systems*, 2023. [1](#), [4](#)

A. Limitations

One limitation of our work is related to the size of cross-attention maps. Smaller maps, particularly those sized 16×16 , contain more semantic information compared to larger maps. While this rich information is beneficial, it restricts our ability to achieve precise and fine-grained structure control. We intend to work on pixel-level text-to-image models to address this limitation. Another limitation is that the frozen Stable Diffusion (SD) model [45] itself lacks straightforward editing capabilities, which may impact the quality of editing results. To address this limitation, we plan to explore ideas from InstructPix2Pix [4] to develop a better text-guided image editing method in the future. Additionally, the SD model faces challenges in reconstructing the original image with intricate details due to the compression mechanism in the first-stage autoencoder model. Editing high-frequency information remains a significant and ongoing challenge that requires further research and development. Overcoming these limitations and advancing our knowledge in these areas will contribute to the improvement and refinement of image editing techniques. Furthermore, it is noteworthy that diffusion models have shown promise across various applications, such as object detection [9], image segmentation [41, 59], and landmark detection [57]. Therefore, a potential future research is to extend diffusion models to various practical applications, including visual tracking, continual learning, font generation, and beyond.

B. Broader Impacts

The application of text-to-image models in image editing has a wide range of potential uses in various downstream applications. Our model aims to automate and streamline this process, saving time and resources. However, it's important to acknowledge the limitations discussed in this paper. Our model can serve as an intermediate solution, accelerating the creative process and providing insights for future improvements. We must also be aware of potential risks, such as the spread of misinformation, the potential for misuse, and the introduction of biases. Ethical considerations and broader impacts should be carefully examined to responsibly harness the capabilities of these models.

C. Dataset statistics

The details of the *COCO-Edit* dataset are presented in Table 3. In this dataset, we have single-object and multi-object images, with seven and six search prompts, respectively. To assess the image editing quality, each search prompt is associated with one editing task, and we compute the average qualitative metrics for evaluation.

D. User Study

In Table 4, we provide the full table of our user studies. Each of the twenty participants was randomly assigned twenty image editing tasks from our *COCO-Edit* dataset. Ten tasks involved single-object images, and the other ten involved multi-object images. Participants were asked to anonymously evaluate the best approach out of six methods based on image editing quality and background preservation. The results show that *LocInv* was preferred by the participants, primarily satisfying their subjective preferences for both single-object and multi-object images. For reference, the user study interface is depicted in Fig. 11.

E. Cross-Attention Maps

In addition to the qualitative and quantitative image editing comparisons presented in the main paper, we have extended our evaluation by including a comparison with full sentences cross-attention maps. These comparisons are illustrated in Fig. 6 and Fig. 7. This comprehensive analysis further demonstrates the superior adaptability and quality of cross-attention maps produced by *LocInv*, in comparison to previous approaches, including NTI [37], DDIM [49], and DPL [53], even across various input prompt lengths and real image scenarios.

F. More Image Editing quality comparison

F.1. Word-Swap

In Fig. 8, we have provided additional qualitative comparisons of image editing with various methods, including DPL[53], as an extension of Fig.4 in the main paper. Among these methods, DPL behaves similarly to NTI [37] in complex real images. However, our method, *LocInv*, exhibits superior image editing quality and background preservation in these comparisons.

F.2. Attribute-Edit

In Fig. 9, we have presented additional Attribute-Edit tasks as an extension of Fig.5 in the main paper. Once again, our method, *LocInv*, stands out as the best approach, successfully achieving attribute modifications such as color and material with superior results.

F.3. Between Segment-Prior and Detect-Prior.

In Fig. 10, we demonstrate that the Segment-Prior of our method *LocInv* achieves improved alignment between the cross-attention maps and the localization priors, also aligning with our expectations. Consequently, the editing performance varies based on the quality of the cross-attention maps, and Segment-Prior outperforms the Detect-Prior based *LocInv* in this regard.

	Prompts	Image Number	Editing task
single-object	airplane	25	airplane → seaplane
	bear	22	bear → panda
	boat	17	boat → canoe
	cat	22	cat → cougar
	elephant	46	elephant → buffalo
	giraffe	37	giraffe → brachiosaurus
	zebra	45	zebra → donkey
multi-object	apple, banana	2	apple → peach
	bench, cat	31	cat → panther
	cat, dog	37	dog → fox
	dog, frisbee	25	dog → raccon
	donkey, zebra	2	donkey → horse
person, dog, boat	4	dog → cat	

Table 3. Comprehensive statistics for the COCO-edit dataset.

User Study (%)							
	method	<i>LocInv</i>	DiffEdit [11]	MasaCtrl [5]	NTI [37]	pix2pix [39]	PnP [52]
Single-Object	Image Editing quality	33.5	33.0	4.5	27.5	0.5	1.0
	Background preservation	20.5	4.0	5.0	22.0	25.0	23.5
Multi-Object	Image Editing quality	46.5	21.0	2.5	23.5	1.0	5.5
	Background preservation	31.0	3.5	4.0	18.0	20.5	23.0
Overall	Image Editing quality	40.0	27.0	3.5	25.5	0.75	3.25
	Background preservation	25.8	3.7	4.5	20.0	22.7	23.3

Table 4. Extended user study with additional statistics over the sing-object and multi-object images separately. Based on the evaluation, it can be inferred that *LocInv* is the best approach, primarily satisfying the evaluators’ subjective preferences for both single-object and multi-object images.

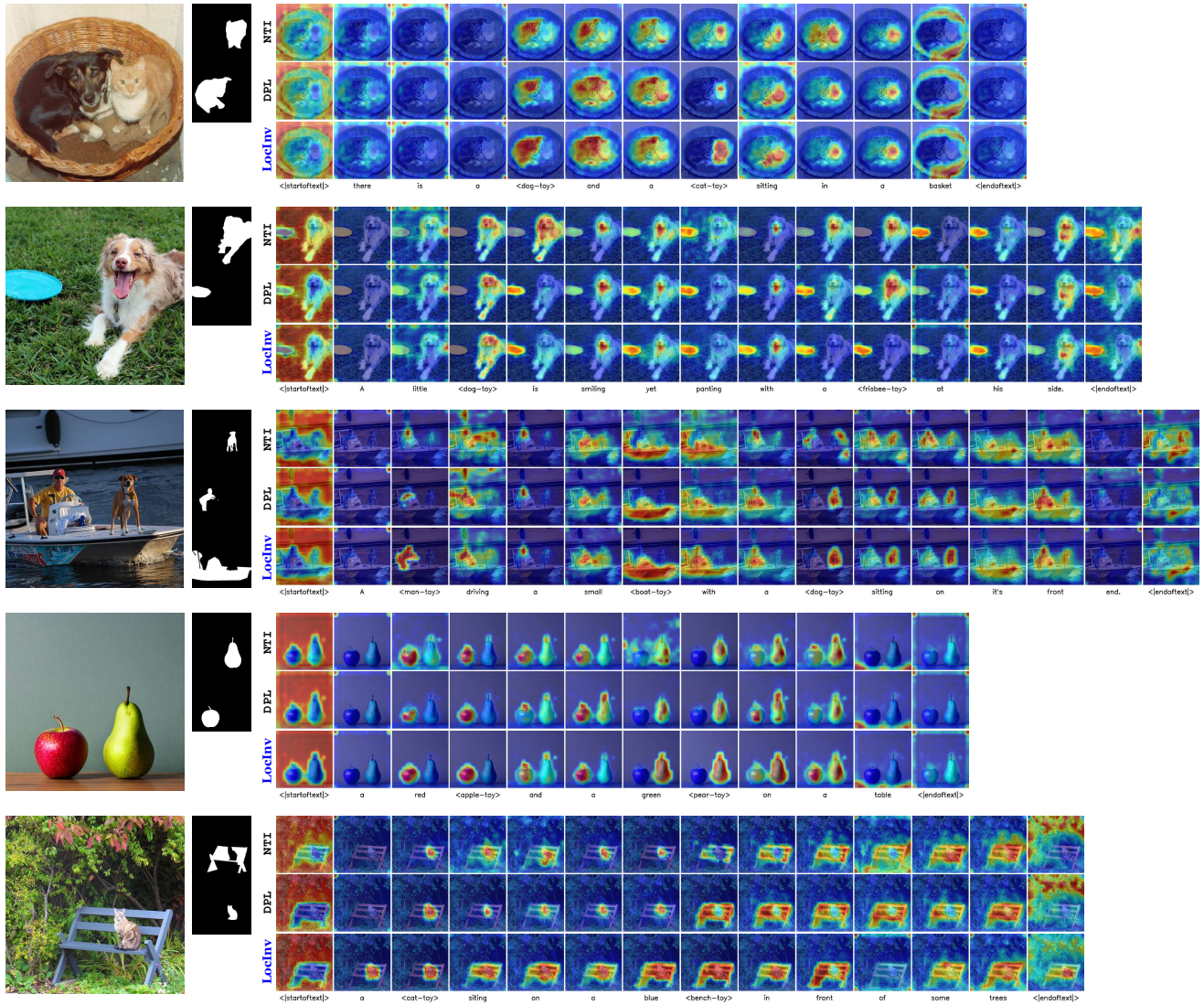


Figure 6. Cross-attention maps are significantly improved by our method, in comparison to previous approaches, including NTI [37], DDIM [49], and DPL [53].

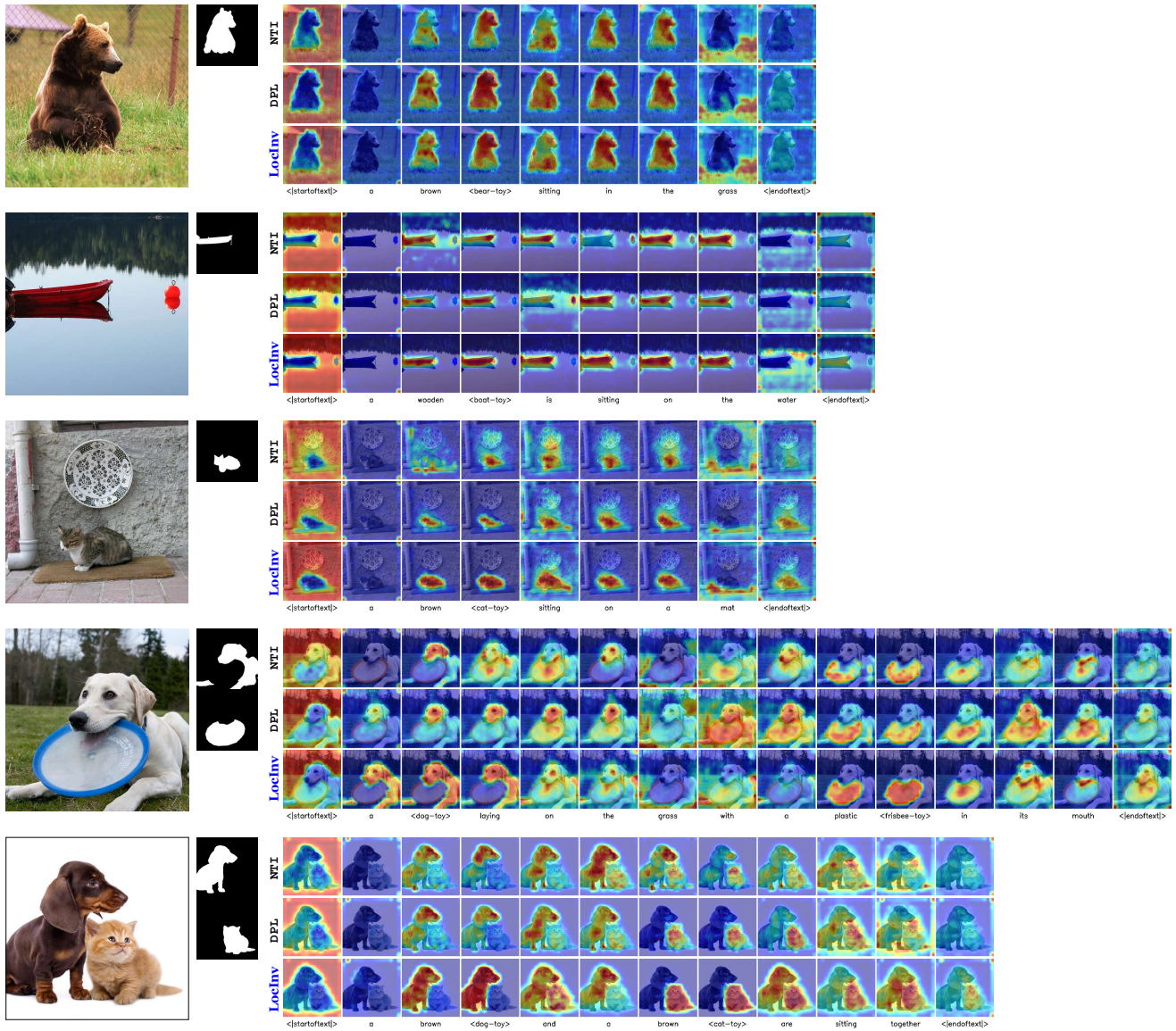
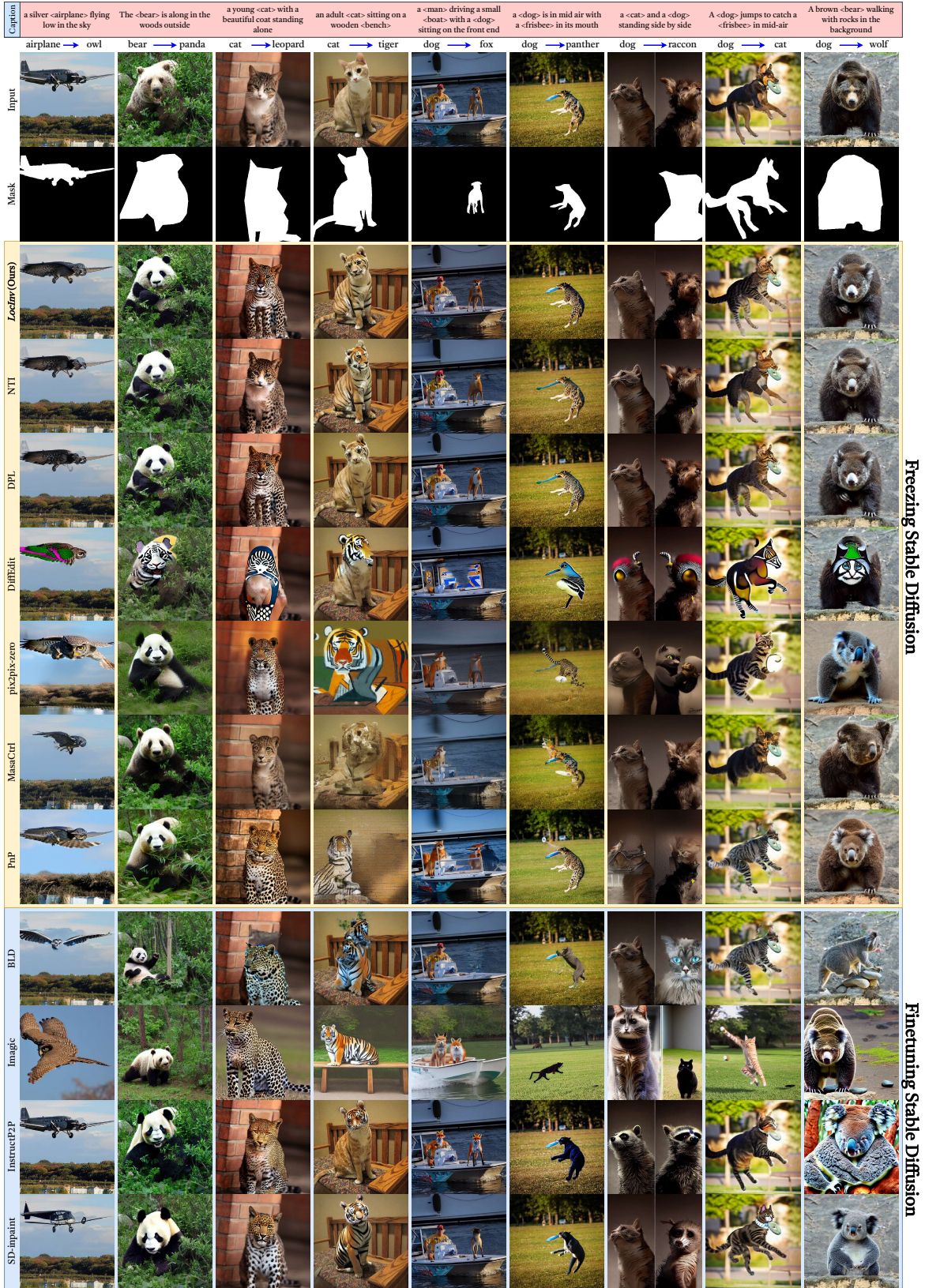


Figure 7. Cross-attention maps are significantly improved by our method, *LocInv*, in comparison to previous approaches, including NTI [37], DDIM [49], and DPL [53].



Freezing Stable Diffusion

Finetuning Stable Diffusion

Figure 8. More comparison examples of the local object Word-Swap editing given the *Segment-Prior*.

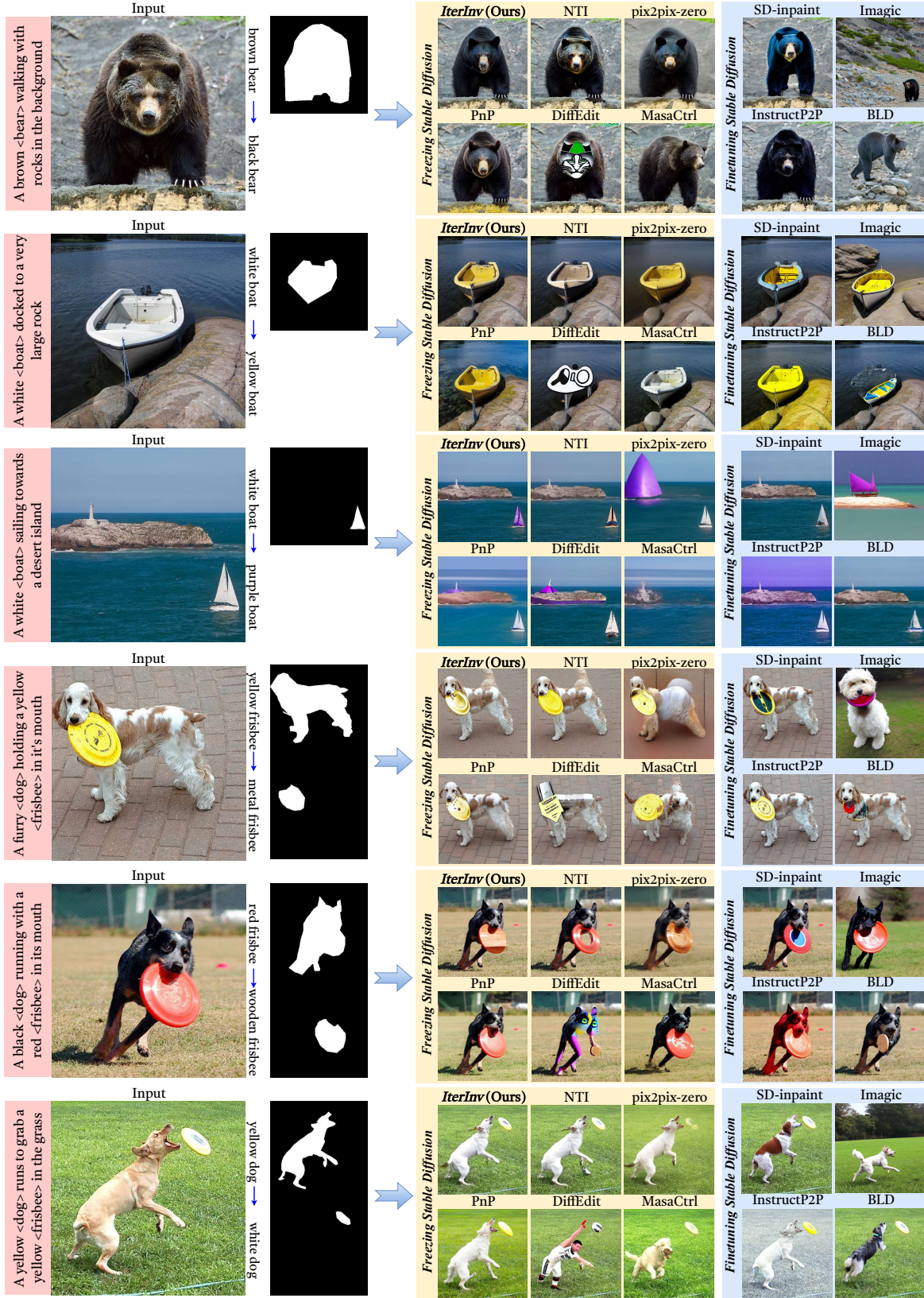


Figure 9. More attribute-Edit with our method *LoInv* by swapping the adjectives given the *Segment-Prior*.

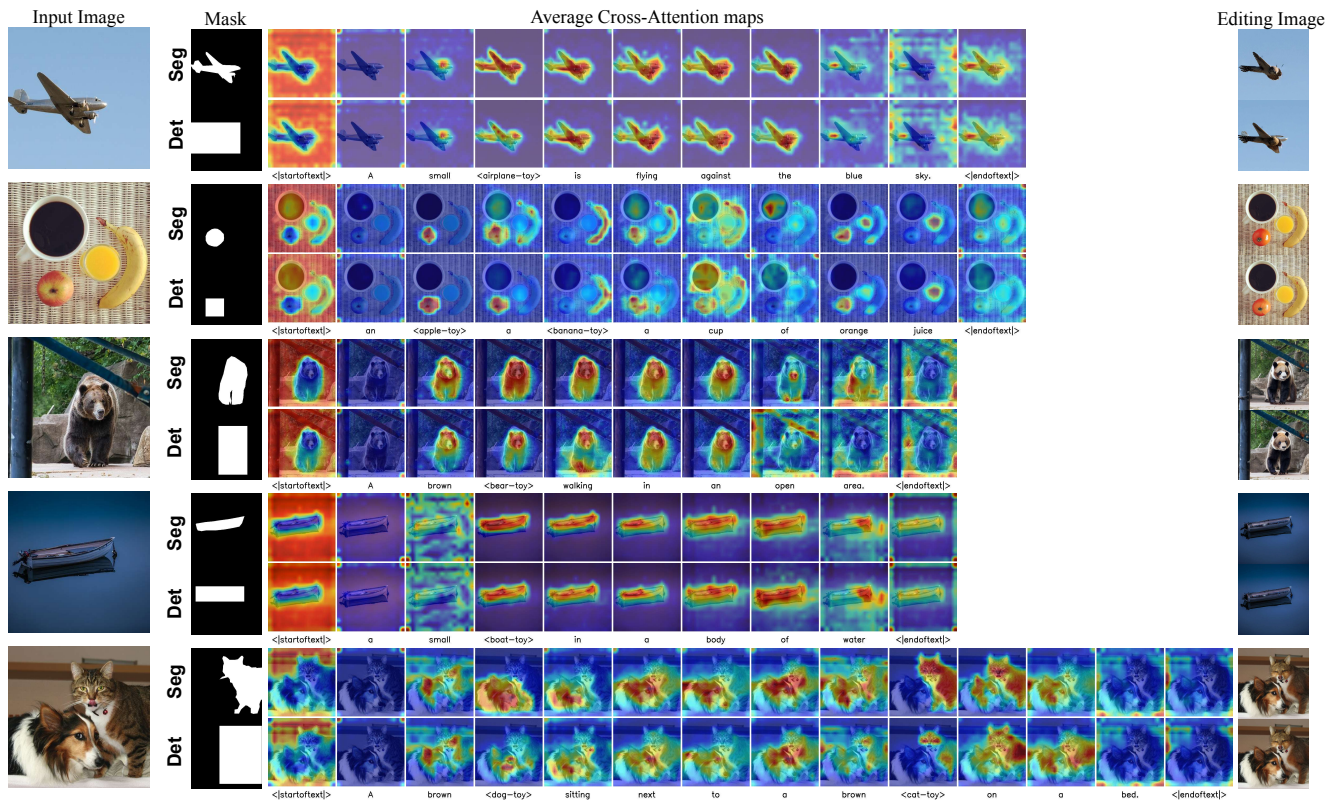


Figure 10. Cross attention maps are better corrected by the Segment-Prior of our method *LoCInv*. The “Seg” and “Det” on the left represent the Segment-prior and Detection-Prior, respectively.

-----Text-Guided Image Editing User Study-----

Hello everyone. We have 20 original images, each with two accompanying questions. Please choose the image that best corresponds to each question. In the six edited images, the object has been changed to a specific target, and the image orders are random. Your opinions and responses to these questions are highly appreciated.



Q1 Editing - In your opinion, which of the above images exhibits the highest semantic translation editing quality for transforming the source object into the target concept? (Considering both image content and style.)

- 1 2 3 4 5 6

Q2 Background - In your opinion, which of the above images best preserves the background and other objects that do not need editing?

- 1 2 3 4 5 6

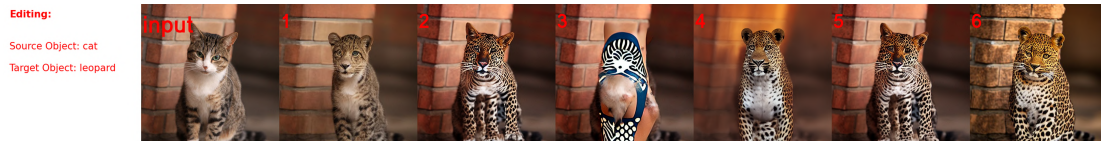


Q3 Editing - In your opinion, which of the above images exhibits the highest semantic translation editing quality for transforming the source object into the target concept? (Considering both image content and style.)

- 1 2 3 4 5 6

Q4 Background - In your opinion, which of the above images best preserves the background and other objects that do not need editing?

- 1 2 3 4 5 6



Q5 Editing - In your opinion, which of the above images exhibits the highest semantic translation editing quality for transforming the source object into the target concept? (Considering both image content and style.)

- 1 2 3 4 5 6

Q6 Background - In your opinion, which of the above images best preserves the background and other objects that do not need editing?

- 1 2 3 4 5 6



Q7 Editing - In your opinion, which of the above images exhibits the highest semantic translation editing quality for transforming the source object into the target concept? (Considering both image content and style.)

- 1 2 3 4 5 6

Q8 Background - In your opinion, which of the above images best preserves the background and other objects that do not need editing?

- 1 2 3 4 5 6

Figure 11. Our user study webpage screenshot.